

Article

Not peer-reviewed version

Screening Health Risks of Trace Metals in Indoor Dust and Settleable Particles in an Industrial Coastal Basin in Chile

[Fiorella González V.](#) , Felipe Lobos O. , Catia Calisto S. , [Ana Valdés D.](#) , [Manuel A. Leiva-Guzmán](#) * , [Richard Toro A.](#) *

Posted Date: 25 February 2026

doi: 10.20944/preprints202602.1458.v1

Keywords: human health risk assessment; indoor settled dust; settleable particulate matter; trace metals; school microenvironments; industrial emissions



Preprints.org is a free multidisciplinary platform providing preprint service that is dedicated to making early versions of research outputs permanently available and citable. Preprints posted at Preprints.org appear in Web of Science, Crossref, Google Scholar, Scilit, Europe PMC.

Copyright: This open access article is published under a [Creative Commons CC BY 4.0 license](#), which permit the free download, distribution, and reuse, provided that the author and preprint are cited in any reuse.

Disclaimer/Publisher's Note: The statements, opinions, and data contained in all publications are solely those of the individual author(s) and contributor(s) and not of MDPI and/or the editor(s). MDPI and/or the editor(s) disclaim responsibility for any injury to people or property resulting from any ideas, methods, instructions, or products referred to in the content.

Article

Screening Health Risks of Trace Metals in Indoor Dust and Settleable Particles in an Industrial Coastal Basin in Chile

Fiorella González V. ¹, Felipe Lobos O. ¹, Catia Calisto S. ¹, Ana Valdés D. ², Manuel A. Leiva-Guzmán ^{1,*} and Richard Toro A. ^{1,*}

¹ Departamento de Química, Facultad de Ciencias, Universidad de Chile, Santiago, Chile

² Centro de Tecnologías Nucleares en Ecosistemas Vulnerables, División de Investigación y Aplicaciones Nucleares, Comisión Chilena de Energía Nuclear, Santiago, Chile

* Correspondence: rtoro81@uchile.cl, manleiva@uchile.cl

Abstract

Industrial coastal basins that host heavy industry can concentrate metal-bearing dust in school environments. We performed a screening multi-matrix assessment across six schools in Quintero-Puchuncaví (central Chile). We measured As, Cd, Cr, Cu, Ni, Pb, and Mn in surface soils (2023 winter only), indoor settled dust, and settleable particulate matter (SPM) collected in winter (July 2023) and summer (November 2023). Concentrations were determined by ICP-OES/ICP-MS and interpreted with enrichment factors and the geoaccumulation index. An U.S. EPA screening framework was used to estimate non-carcinogenic hazard (HQ) and incremental lifetime cancer risk (ILCR) for ingestion, inhalation, and dermal contact, as well as general assessment for non-carcinogenic risk (HI) and carcinogenic risk (*Risk*). SPM carried the strongest anthropogenic signal (EF up to 9900 for Cd, 408 for Cu, and 143 for Pb) and the highest summer loads (Cu >5000 mg kg⁻¹; Ni >1000 mg kg⁻¹). Cu dominated non-carcinogenic hazard (HQ up to 137), whereas ILCR was driven by Ni, As, and Cr, exceeding 10⁻⁴ and reaching 10⁻³ at inland schools in summer. Indoor dust showed intermediate burdens, indicating indoor accumulation of outdoor-derived metals, while soils acted as longer-term reservoirs. Despite the limited sample size, the results motivate emission control, dust mitigation in schools, and targeted follow-up monitoring.

Keywords: human health risk assessment; indoor settled dust; settleable particulate matter; trace metals; school microenvironments; industrial emissions

1. Introduction

Industrial development has supported economic growth, yet it has also intensified environmental degradation and associated health inequities [1, 2]. Industrial sources emit trace metals (TMs) and particulate matter (PM) that can persist in the atmosphere and accumulate in outdoor soils and indoor reservoirs such as settled dust [1, 3, 4]. Metals span a wide particle-size range; fine fractions contribute to inhalation exposure, whereas coarse and settleable fractions deposit to surfaces and are readily transferred indoors [3, 4]. Children are particularly susceptible because exposure factors (higher intake per unit body mass and frequent hand-to-mouth activity) coincide with developing respiratory and neurological systems [4].

Across urban and industrial settings, studies report enrichment of toxic metals in street dust, school dust, and deposited particulate matter, often accompanied by screening-level non-carcinogenic and carcinogenic risks [5-8]. These findings support evaluating both outdoor deposition and indoor accumulation, because settled dust is easily contacted and inadvertently ingested during routine school activities [4-8].

International guidance identifies particulate pollution as a major environmental risk factor and has tightened guideline values for PM_{2.5} and PM₁₀, with explicit attention to vulnerable groups [9, 10]. Public-health agencies also stress that no safe level of lead exposure has been identified for children, and that legacy reservoirs such as soil and dust can sustain exposure even when emissions change [11]. Accordingly, characterizing contaminant sources in and around schools located near industrial facilities is a priority for exposure reduction [9-11].

The term environmental “sacrifice zone” is a ‘theoretical’ category used to identify and address inequalities caused by excessive industrial development at the expense of the environment, resulting in socio-environmental disasters [12, 13]. The populations affected are often low-income and reside in areas heavily impacted by chemical pollution, living adjacent to highly contaminated industries or military bases [14]. This framing emphasizes that exposure is shaped not only by emissions, but also by land-use decisions and unequal regulatory protection, and it is often used by affected communities to demand remediation and structural change [15, 16]. There are several sacrifice zones around the world; however, the greatest increases have occurred in peripheral countries in Africa, Asia, and Latin America [17].

Quintero–Puchuncaví, on the central coast of Chile, hosts a dense industrial corridor that includes thermoelectric generation, oil refining, petrochemical operations, port activities and used to include copper smelting [18-21]. Atmospheric deposition and soil surveys in the district report elevated concentrations of Cu, As, Pb, and other elements, consistent with sustained industrial influence and local topographic confinement [18-21]. In schools, indoor settled dust and settleable particulate matter (SPM) provide integrative media linking outdoor deposition, infiltration, and resuspension, and they are relevant to ingestion, inhalation, and dermal exposure pathways [3, 21, 22]. Recent school-based evidence further supports the public-health and environmental-justice relevance of this setting [22].

Despite a growing literature on soils, atmospheric deposition, and air quality in the district, evidence remains fragmented across media and seasons [18-22]. Few assessments combine soils, indoor dust, and deposited particulate matter within the same schools, limiting inference on soil-to-dust transfer and indoor accumulation [18-21]. In addition, multi-pathway risk assessments that jointly consider ingestion, inhalation, and dermal contact remain scarce for schoolchildren in this setting [21, 22].

To address these gaps, we applied a screening multi-matrix assessment across six schools, measuring As, Cd, Cr, Cu, Ni, Pb, and Mn in surface soils, indoor settled dust, and SPM collected in winter and summer. We evaluated enrichment using EF and Igeo and estimated non-carcinogenic hazard and incremental lifetime cancer risk for ingestion, inhalation, and dermal contact using U.S. EPA screening equations [23-26]. The aim is to provide an exposure-oriented evidence base for school-level mitigation and local environmental management in an industrial coastal basin.

2. Materials and Methods

2.1. Study Area Description

The towns of Quintero and Puchuncaví are located on the central coast of Chile (32°45'S, 71°28'W), about 160 km northwest of Santiago and 50 km north of Valparaíso. The area lies within the coastal plain, bounded by the Pacific Ocean and the coastal mountain range. Its geography and topography-low-elevation terraces and valleys that funnel winds inland-restrict pollutant dispersion and favor the accumulation of emissions. Climatically, it is characterized by a Mediterranean coastal regime with mild winters, cool summers, and low annual rainfall (~350–400 mm) [27], with prevailing southwesterly winds and frequent thermal inversions that trap pollutants near the surface. These features, combined with limited precipitation, enhance the deposition and resuspension of PM and TMs.

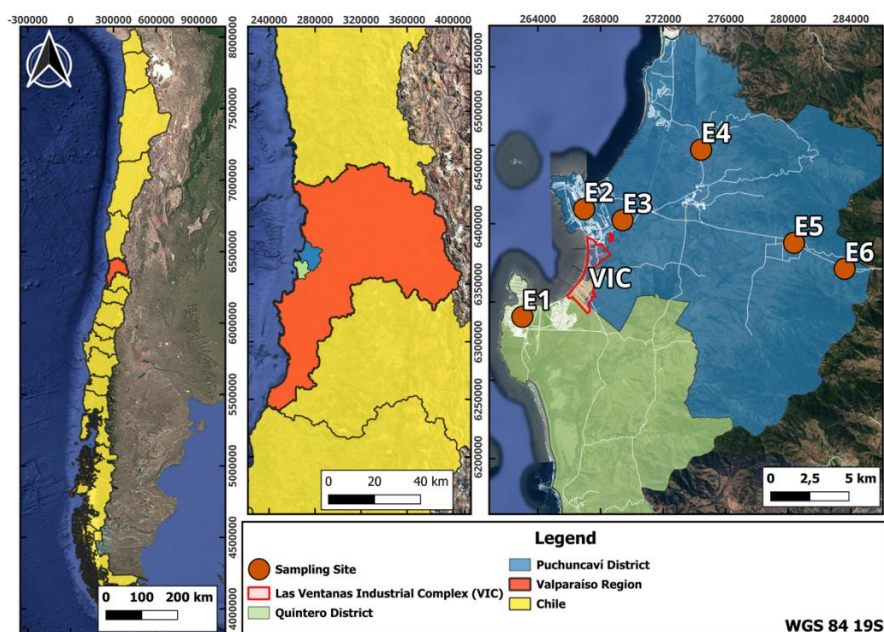


Figure 1. Location of the study area in central Chile. The map shows the Valparaíso Region's position within Chile (left), the Quintero and Puchuncaví districts' locations (center), and the Las Ventanas Industrial Complex (VIC) polygon, the school sampling sites (E1–E6), and the urban areas highlighted in white (right).

Economically, the district has undergone a marked shift toward heavy industry since the 1960s, with major installations in energy production, refining, and mining-related processing. Traditional livelihoods such as agriculture, livestock, and artisanal fishing persist, but they coexist with an industrial landscape that has reshaped land use and local exposure pathways.

Monitoring and case reports describe recurrent exceedances of air-quality standards and episodic acute intoxication events in the district [28]. Surveys of soils and sediments report enrichment of As, Pb, Cu, and Cd, in some cases exceeding health-based guideline values [18, 19, 22]. Ecological impacts have also been reported, including changes in seaweed, mollusk, and fish populations [29].

These long term exposure to high concentrations of air pollutants characterize Quintero–Puchuncaví as a sacrifice zone. Although recent developments lead to the closure of the copper smelter of CODELCO División Ventanas in June of 2023 [17], historically there has been a prioritization of industrial activity and energy production over public health protection [2, 30, 31].

Quintero–Puchuncaví therefore represents an environmental-justice case in which concentrated industrial emissions intersect with residential proximity and uneven regulatory safeguards.

2.2. Sampling Descriptions

Sampling was conducted at six educational establishments (E1–E6; see Figure 1) in the Quintero–Puchuncaví district. República de Francia School (E1) is located in Quintero, while La Chocota (E2), La Greda (E3), Escuela Básica El Rungue (E4), Pucalán (E5) and Los Maquis (E6) are located in the Puchuncaví sector. The results for each site were identified according to the numerical designation assigned to each school.

Two campaigns were designed to capture seasonal contrasts: winter (July 2023) and summer (November 2023). To indicate the corresponding season, results are labeled using the letters W and S for winter and summer, respectively. Since soil samples were obtained only during the winter campaign, no seasonal distinction is applied to soil sample results. Each sample was collected during dry weather to minimize washout effects and to represent conditions typical of the region's Mediterranean coastal climate.

Three environmental matrices were evaluated: surface soils, indoor settled dust, and outdoor settleable particulate matter (SPM), representing major exposure media for schoolchildren. Soil samples (coded "S") were collected during the winter campaign from four schools (E1–E4). Between three and five samples were taken per school. Surface soil was sampled from playgrounds and high-traffic areas using a plastic spatula, stored in resealable polyethylene bags, and transported under cooled conditions. In the laboratory, soils were air-dried (<25 °C) and sieved to <63 µm nylon mesh to isolate the fine fraction most relevant to ingestion and resuspension.

One indoor dust sample (labeled "D") was collected per school using a plastic spatula from high furniture or other indoor surfaces and stored in sealable plastic containers. SPM samples (labeled "P") were collected using a passive sampler constructed according to the specifications of the University of North Carolina (UNC) passive aerosol samplers [32] fitted with nucleopore filters Whatman 111111. One sampler was deployed per school in open areas, avoiding wind obstructions whenever possible. Unlike soil and dust, which were collected in a single day, passive SPM samplers remained in place for about one month.

Following this sample and seasonal identification methodology, results are reported using alphanumeric codes that combine matrix type, sampling season, and site number. For example, winter indoor dust results from La Chocota School are identified as DW2, whereas a soil sample result from Los Maquis School is identified as S6. A summary of the sampling process can be found in Supplementary Table S1.

Quality assurance and quality control procedures were implemented throughout sampling and handling. Equipment was acid-washed (10% HNO₃) and rinsed with ultrapure water; personnel wore powder-free nitrile gloves and avoided metallic tools. Samples were labeled with alphanumeric codes, georeferenced (±5 m GPS), and accompanied by chain-of-custody records. Meteorological data (temperature, wind speed/direction, precipitation) from the Chilean Meteorological Directorate were used to contextualize conditions during SPM exposure [27].

2.3. Sample Preparation and Chemical Analysis

All samples were processed in the Environmental Chemistry Laboratory of the University of Chile under strict chain-of-custody conditions. Soils and dust were air-dried at room temperature and sieved to <63 µm. SPM filters were handled in a laminar-flow hood, sectioned as needed, and prepared directly for digestion.

Microwave-assisted acid digestion was used to extract metals from all matrices in PTFE vessels with 10 mL of high-purity nitric acid. For soils and indoor dust, digestion followed a standard program consistent with Method 3051A, using 6–9 mg per sample [33]. For polycarbonate filters (SPM), a staged program with an initial low-power step was applied to avoid rapid exothermic reactions and to achieve complete mineralization, following Dos Santos Souza et al. [34]. After digestion, solutions were filtered through 0.45 µm PTFE membranes and diluted with ultrapure water up to 50 mL for ICP-MS analysis. Reagent blanks were processed with each batch to verify cleanliness, and all materials were thoroughly cleaned following standard procedure: 10 standard rinses with distilled water, followed by 10 rinses with ultrapure water. Subsequently, the materials were soaked in a 10% (v/v) HNO₃ solution for 48 hours [33, 34]. The digestion programs are summarized in Table 1.

Table 1. Summary of acid digestion program for microwaved assisted acid digestion used for soil, indoor dust and PM samples.

Sample Matrix	Solution (mL)	Step s	Power (W)	Ramp temperature (°C)	Ramp time (min)	Max. Pressure (Bar)	Temperature (°C)	Time (min)
Soil / Indoor Dust	10 HNO ₃ Suprapur	1	960	175±5	5.5±0.25	S/I	175±5	4.5

Particulate Matter	10 HNO ₃ Suprapur	1	500	120	8	S/I	120±5	10
		2	800	180	5		180±5	8

Quality assurance for soil samples was possible thanks to support of the Chilean Commission of Nuclear Energy (abbreviated CCHEN in Spanish). Although, due to security reasons, results were not provided, CCHEN assured the acid digestion process was successful.

2.4. Environmental Impact Assessment

To screen for anthropogenic influence and to compare contamination intensity across matrices, we calculated enrichment factors (EF) and the geoaccumulation index (I_{geo}). These indices relate measured concentrations to background levels and provide a standardized basis for interpreting enrichment and contamination in soils, indoor dust, and deposited particulate matter.

The enrichment factor (EF) was calculated as the ratio of the concentration of each element to a reference element in the sample, normalized by the same ratio in background soils. Manganese (Mn) was selected as the reference element because of its geochemical stability, low mobility, and minimal anthropogenic enrichment in the region [35]. EF values were interpreted using standard classes ranging from minimal enrichment (EF < 2) to extremely high enrichment (EF > 40) [35].

The geoaccumulation index (I_{geo}), originally proposed by Müller [36], was used to quantify contamination relative to background by computing the base-2 logarithm of the ratio between the measured concentration (C_m) and 1.5 times the background concentration (B_m). The factor 1.5 accounts for natural variability in background levels. I_{geo} was classified into seven categories from uncontaminated (I_{geo} ≤ 0) to extremely contaminated (I_{geo} ≥ 5) [37, 38]. Background concentrations were obtained from a baseline dataset for the Quintero–Puchuncaví district derived using a median absolute deviation (MAD) approach [39], these values can be found in Supplementary Table S2. For EF normalization, the measured Mn reference concentration in soils (C_{ref, Mn}) was 834 ± 223 mg/kg, consistent with local natural conditions.

Numeric labels within cells indicate measured EF or I_{geo} values, formatted with one decimal place if <10 and rounded integers if ≥10.

2.5. Health Risk Assessment (HRA)

The health risk assessment was conducted in accordance with EPA guidelines and used default exposure factors. Key scenario parameters are summarized in Table 2. Further details on the assumptions and parameters used are available in Supplementary Text 1 and Table S3. Two main assumptions were applied: all exposures were chronic, and all samples were treated as dust. Specifically, SPM and soil samples were each assumed to represent dust composed exclusively of one of these materials. This approach aimed to assess scenarios where highly polluted SPM or soil predominates the ID composition, allowing comparison with actual ID samples.

Table 2. Values used for the risk assessment calculations [22, 23, 25, 26, 40-43].

Variable	Meaning	Children	Children	Adolescents/adults
		(<6 ages)	(6–12 ages)	(12–80 ages)
C _m (mg/kg)	Concentration per sample	Concentration per sample		
I _{ngR} (mg/day)	Ingestion Rate	100	60	60
I _{nhR} (m ³ /day)	Inhalation Rate	13.8	16.6	24.6

SA (cm ²)	Exposed Skin Surface	2800	5700	5700
SF (mg/cm ²)	Soil-Skin Adherence Factor	0.2	0.2	0.07
ABS (%) [As]	Dermal Absorption Factor		0.03	
ABS (%) [Other]	Dermal Absorption Factor		0.001	
EF (day/year)	Exposure Frequency	Soil: 10; Dust: 50; SPM: 60	Soil: 10; Dust: 57; SPM: 67	Soil: 14; Dust: 89; SPM: 102
ED (year)	Exposure Duration	5	3.5	30.5
CF (kg/mg)	Conversion factor		1·10 ⁻⁶	
PEF (m ³ /kg)	Particulate Emission Factor		1.36·10 ⁹	
BW (kg)	Body Weight	10.8	45.6	106.5
ATnc (days)	Average time (AT) for non-carcinogenic effects to manifest		ED x 365	
ATca (days)	Average time (AT) for carcinogenic effects to manifest		80 years x 365	

All samples were treated like solid samples, because of this the estimated ingestion (I) per exposition route for all samples were calculated using equations 3, 4 and 5. For the assessment of health risk, Hazard Quotient (HQ) and Hazard Index (HI) were used to evaluate non-carcinogenic effects. For assessment of carcinogenic effects Incremental Lifetime Cancer Risk (ILCR) and Risk index (Risk) were used. The equations used correspond to 6, 7, 8 and 9 respectively.

$$I_{Ingestion} = \frac{C_m \cdot I_{ng} R \cdot EF \cdot ED}{BW \cdot AT} \cdot CF \quad (3) \quad I_{Inhalation} = \frac{C_m \cdot I_{nh} R \cdot EF \cdot ED}{BW \cdot PEF \cdot AT} \quad (4)$$

$$I_{Dermic} = \frac{C_m \cdot SA \cdot SF \cdot ABS \cdot EF \cdot ED}{BW \cdot AT} \cdot CF \quad (5)$$

$$HQ = \frac{I}{RfD} \quad (6) \quad HI = HQ_{Ingestion} + HQ_{Inhalation} + HQ_{Dermic} \quad (7)$$

$$ILCR = I \cdot SF \quad (8)$$

$$Risk = ILCR_{Ingestion} + ILCR_{Inhalation} + ILCR_{Dermic} \quad (9)$$

Where C_m it's the concentration of the element per sample (mg/kg) and n represents the age groups used for HRA. Following the recommendations made by the EPA to identify potentially unrealistic exposure scenarios or overestimated risks [23-25], values of HQ or ILCR that substantially

deviated from their respective reference values were excluded from the analysis of HI and Risk respectively. To assess the overall risk for the sampled area, the indices HI and Risk are summed. To facilitate overall interpretation, HQ and HI two times higher than the threshold (value of 1) were presented with decimals. Standard values used for the assessment are provided in Tables 2 and 3.

Table 3. Reference Dose (RfD) values (mg/(kg·day)⁻¹) and Slope Factor (SF) for each TE [40, 44-46].

TE	RfD _{ing}	RfC	RfD _{derm}	SF _{ing}	SF _{inh}	SF _{Der}
As	3.0·10 ⁻⁴	1.5·10 ⁻⁵	1.2·10 ⁻⁴	1.5	1.51	3.7
Cd	5.0·10 ⁻⁴	1.0·10 ⁻⁵	1.0·10 ⁻⁵	-	6.3	-
Cr	3.0·10 ⁻³	1.0·10 ⁻⁴	6.0·10 ⁻⁵	0.5	4.2	2
Cu	3.0·10 ⁻⁴	-	1.2·10 ⁻²	-	-	-
Ni	2.0·10 ⁻²	9.0·10 ⁻⁵	5.4·10 ⁻³	1.7	0.9	4.25
Pb	4.3·10 ⁻⁴	1.5·10 ⁻⁴	5.3·10 ⁻⁴	8.5·10 ⁻³	4.2·10 ⁻²	-

2.6. Statistical and Computational Tools

All statistical analyses were performed in R (v4.3.4). Descriptive statistics (mean, standard deviation, relative standard deviation, and 95% confidence intervals) were computed for each matrix and campaign. Because concentration distributions were non-normal and heteroscedastic, non-parametric tests (Mann–Whitney U; Kruskal–Wallis) were used for comparisons across matrices and seasons.

Pairwise comparisons were performed to assess statistically significant differences in the concentrations of the six TMs among the sample types (particulate matter, soil, and indoor dust). Analyses were conducted using R (v4.3.4) in RStudio.

Outliers were removed using the IQR method. Normality was assessed using the Shapiro–Wilk test, and non-parametric Wilcoxon rank-sum tests were applied for pairwise comparisons of the TMs. To control for Type I error, a Bonferroni correction was applied.

To enable pairwise comparisons among soil, PM, and ID samples, it was assumed that the soil samples represented the overall sampling area. This assumption was necessary due to spatial constraints in soil sampling and justified treating the sample types as dependent based on shared area of origin rather than specific sampling points.

Post hoc pairwise comparisons were conducted using Dunn’s test with Bonferroni adjustment to control family-wise error. For these analyses, soil samples were treated as representative of the overall study area, acknowledging spatial constraints in soil sampling and the shared origin of the matrices.

Certainty bands were used to evaluate the level of certainty for the SPM and indoor dust results. Detailed descriptions of the methodology used to determine the ranges of the bands and the associated certainty criteria can be found in Supplementary Text 2 and Tables S4–S7.

3. Results and Discussion

3.1. Elemental Concentrations and Spatiotemporal Variability

Table 4 reports mean (±SD) concentrations of As, Cd, Cr, Cu, Ni, and Pb across soils, indoor dust, and SPM. TMs concentrations were generally the highest in SPM samples, which exhibited the highest per-sample maxima and average values across both sampling campaigns, followed by dust and soil. However, in schools E1 and E2, soil samples showed higher concentrations than indoor dust, deviating from the general trend.

Seasonal and spatial variability in elemental concentrations for all types of samples was reflected in all the indices obtained.

In SPM samples, As, Cd, Cr, and Ni concentrations were higher during the warm season, while Cu and Pb peaked in the cold season. Schools E5 and E6 showed increased levels of all metals in summer. In ID, As, Cr, Cu, and Pb concentrations were generally higher in summer, while Cd and Ni exhibited no consistent seasonal pattern across sites. Unlike SPM, dust samples did not show a uniform increase in all metals during summer at any location.

As a general case spatial variability was pronounced, particularly in SPM, as reflected by high standard deviations and relative standard deviations. The Supplementary Material (Supplementary Table S8) provides site-level values and shows that schools E5 and E6, located in coastal valleys downwind of the Ventanas complex, had the highest SPM concentrations.

Table 4. Average concentrations of TMs (mg kg^{-1} , mean \pm SD) in settleable particulate matter (SPM), indoor dust, and soils collected from schools in Quintero–Puchuncaví during winter (W) and summer (S) campaigns.

Sample type	As	Cd	Cr	Cu	Ni	Pb
SPM – Winter (PW)	90.8 \pm 37.6	80.9 \pm 74.3	296.5 \pm 157.4	4337.6 \pm 1997.5	317.7 \pm 159.4	377.7 \pm 195.5
SPM – Summer (PS)	469.4 \pm 615.5	340.6 \pm 457.2	1338 \pm 1579.5	5328.3 \pm 6902.9	1025.1 \pm 1316	706.8 \pm 923.5
Indoor dust – Winter (DW)	31.5 \pm 20.1	3.2 \pm 0.6	67.3 \pm 29.2	689.5 \pm 511	84.6 \pm 50	94.5 \pm 51.5
Indoor dust – Summer (DS)	30.4 \pm 10.4	3.8 \pm 2.0	116.5 \pm 136.6	860.5 \pm 521.3	77.3 \pm 39.7	141.1 \pm 52.6
Soil (Sites E1-E4) (S)	26.3 \pm 10.0	5.7 \pm 3.0	70.4 \pm 43.0	443.6 \pm 387.4	57.7 \pm 19.0	82.9 \pm 32.6

The seasonal divergence suggests that summer increases are linked to enhanced resuspension and dry deposition of contaminated material, whereas wintertime conditions may reflect differences in emission patterns and atmospheric processing for Pb- and Cu-bearing particles [1]. Pairwise comparisons (Supplementary Table S10) are consistent with these patterns. There were no statistically significant differences between indoor dust and SPM samples, in contrast, significant differences were observed between indoor dust and soil samples for almost all TMs (exception being Cr, for which no statistically significant difference was found). These results suggest that the primary source of TMs in ID is airborne PM. Consequently, the deposition of SPM appears to be the most significant contributing process.

The dynamics between indoor dust and SPM, and the weaker seasonality exhibited by indoor dust, are consistent with longer integration times indoors. This is associated with mechanisms that promote particle deposition onto indoor surfaces, such as advection and turbulent diffusion, which are typically strong enough to rapidly transport particles from the atmosphere to surfaces [3].

By contrast, soils and indoor dust were often more similar, suggesting that soil-to-dust transfer occurs indirectly through resuspended particulate matter rather than direct contact, and shows it's comparatively stable and likely act as long-term reservoirs that feed SPM and dust through wind-driven resuspension. Overall, SPM emerges as the most dynamic and contaminated medium, while indoor dust represents the interface most directly connected to children's exposure in schools.

3.2. Enrichment Factor and Geoaccumulation Index

Figure 2 summarizes EF and Igeo values for SPM, indoor dust, and soils across the district. Cadmium (Cd) exhibited the strongest enrichment, with EF values reaching 9905 and Igeo indicating heavily to extremely contaminated conditions at several sites. These results imply Cd concentrations more than two orders of magnitude above background and are consistent with reports from other industrially impacted environments [5, 6].

Copper (Cu) also showed persistent enrichment, with EF values ranging from 16 to 408 in SPM and Igeo reaching class 4. This pattern is consistent with long-term contributions from copper

smelting and related metallurgical activities in the district, where Cu is a major emitted element [19–21]. Resuspension under dry and windy conditions likely redistributes Cu-rich particles, facilitating transfer into indoor environments.

Lead (Pb) showed marked enrichment, with EF as high as 143 and Igeo up to 5.9 in summer SPM (PS6), consistent with strong anthropogenic influence. This signal aligns with contributions from copper smelting and associated industrial processes reported for the district [19–21]. Because Pb is strongly retained in soils and dust, legacy deposits can sustain exposure through erosion and resuspension even as primary emissions change [4, 47].

Arsenic (As) exhibited moderate to high enrichment (EF = 6–21 in SPM), with Igeo values up to class 3, indicating moderate to strong contamination. Although less extreme than Cd or Cu, these levels are relevant given the established carcinogenicity of As via inhalation and ingestion [48]. Chromium (Cr) showed lower average enrichment but reached EF values up to 120 at localized hotspots, indicating spatially heterogeneous contributions.

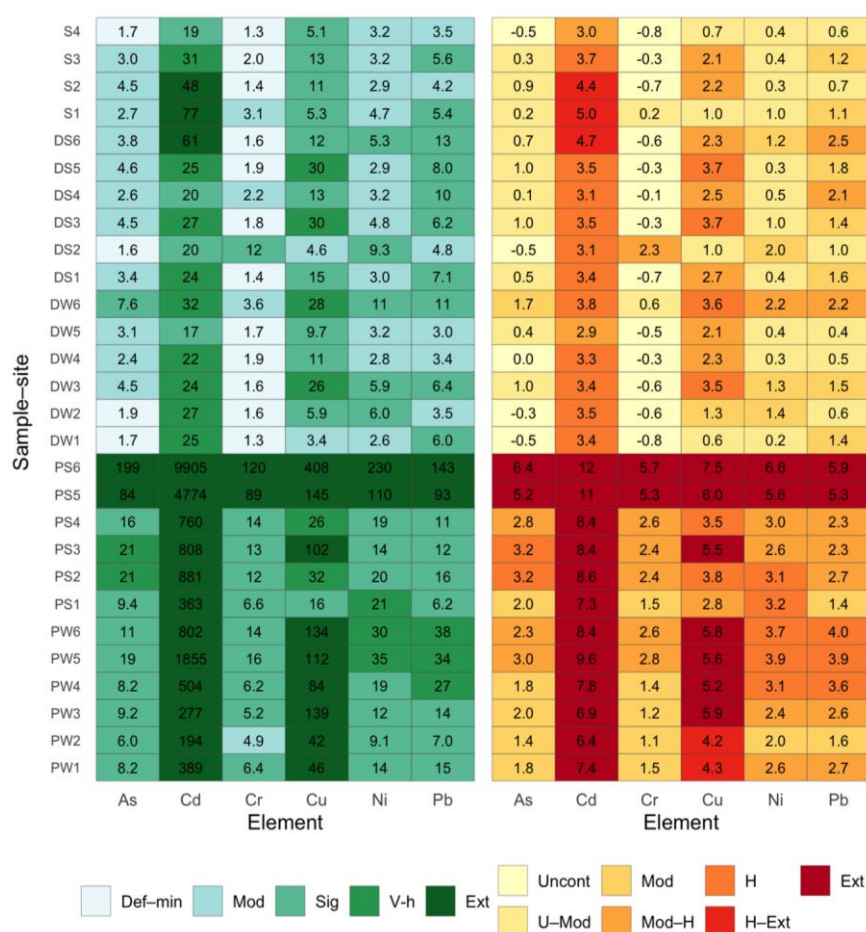


Figure 2. Heatmap visualization of Enrichment Factor (EF, left) and Geoaccumulation Index (Igeo, right) values for six TMs (As, Cd, Cr, Cu, Ni, Pb) across different sample sites in the Quintero–Puchuncaví district. Sampling included surface soils (S1–S4), indoor dust (DS1–DS6; DW1–DW6), and settleable particulate matter (PS1–PS6; PW1–PW6). Values are color-coded according to contamination categories: EF (Def–min = deficiency to minimal enrichment, Mod = moderate, Sig = significant, V–h = very high, Ext = extremely high) and Igeo (Uncont = uncontaminated, U–Mod = uncontaminated to moderately contaminated, Mod = moderately contaminated, H = heavily contaminated, Mod–H = moderately to heavily contaminated, H–Ext = heavily to extremely contaminated, Ext = extremely contaminated). Numeric labels within cells indicate measured EF or Igeo values, formatted with one decimal place if <10 and rounded integers if ≥ 10 .

The comparatively lower enrichment of Cr and Ni in soils relative to SPM likely reflects a combination of background contributions and source-dependent partitioning across particle sizes. In

the Quintero–Puchuncaví coastal environment, soil acidification and salinization linked to industrial activity can influence TMs mobility and redistribution. Seasonal amplification was evident in SPM, with EF and Igeo for Cd, Cu, and Ni peaking in summer, when drier conditions and stronger winds enhance resuspension and transport [20, 27]. These effects were most pronounced in coastal valleys, where topographic constraints limit ventilation and favor contaminant accumulation [20, 21].

By comparison, soils generally exhibited lower enrichment ($EF < 10$ for most metals), although Cd still reached very high values at specific sites. Even with lower EF, soils function as longer-term reservoirs and can contribute to airborne contamination via resuspension. Indoor dust, in turn, integrates outdoor inputs and concentrates them in enclosed environments, which is especially relevant in schools where children spend prolonged periods.

3.3. Health Risk Assessment

Table 5 and Table 6 summarize screening non-carcinogenic hazards and carcinogenic risks for each matrix and season. For SPM, copper dominated non-carcinogenic hazard, with Cu HQ ranging from 5.0 at PS1 to 137 at PS6—well above the $HQ = 1$ benchmark. Even when Cu is excluded from HI and ΣHI to avoid masking other metals, SPM retained elevated cumulative hazard. In summer, HI peaked at 39 (PS6) and 21 (PS5), compared with a winter maximum of 4 (PW4). Soils yielded HI values < 1 across sites (maximum = 0.84 ± 0.68 at S3). Indoor dust showed intermediate hazard, consistent with its role as a conduit between outdoor deposition and indoor exposure.

Because Cu dominates the hazard profile, Table 2 reports HI and ΣHI excluding Cu for SPM and indoor dust, while Cu HQ values are shown separately. When Cu is included ($HI_{total} = HI + HQ_{Cu}$), total hazard ranges from 15–50 for winter SPM (PW1–PW6) and 7–176 for summer SPM (PS1–PS6), and from 2–10 for winter dust (DW1–DW6) and 4–10 for summer dust (DS1–DS6).

A consistent hierarchy of element contributions emerged across matrices. In SPM, Cu exceeded non-carcinogenic thresholds by more than two orders of magnitude at the most impacted sites. Lead and arsenic also contributed substantially, reaching HQ values of 12 and 7, respectively, at valley schools (PS5–PS6). Cadmium and chromium contributed at lower levels but remained non-negligible in SPM and dust. Soil HQ values were generally < 0.1 , indicating comparatively low direct-contact hazard. Indoor dust acted as an intermediate medium, with HI values at or near unity in several schools, reflecting accumulation and resuspension within classrooms.

Carcinogenic risk estimates show a different pattern. SPM was the dominant carcinogenic medium, with Ni, As, and Cr exceeding 1×10^{-4} in summer at valley schools (PS5–PS6). Maximum ILCR values reached 8.9×10^{-4} (Ni), 4.9×10^{-4} (As), and 2.9×10^{-4} (Cr), which correspond to “probable cancer risk” scenarios under U.S. EPA screening guidance. Soils were one to two orders of magnitude lower (typically 10^{-6} – 10^{-5}). Indoor dust contributed measurably, with $\Sigma Risk$ slightly exceeding 1×10^{-4} in summer. The carcinogenic ranking (Ni > As > Cr > Pb > Cd) reflects toxicity rather than absolute concentration, whereas Cu drives non-carcinogenic hazard but contributes little to carcinogenic risk. At the least impacted schools (E1–E2), ILCR remained $< 10^{-6}$ across matrices, indicating negligible carcinogenic risk.

Seasonal and spatial gradients provide additional context. For SPM, ΣHI increased from 21 in winter to 73 in summer, and $\Sigma Risk$ increased from 7.5×10^{-4} to 3.1×10^{-3} . This summer amplification is consistent with drier conditions and stronger winds that enhance soil resuspension and particulate transport. Spatially, valley schools (PS5–PS6) showed up to tenfold higher ΣHI and $\Sigma Risk$ than coastal schools, consistent with pollutant accumulation under topographic confinement.

Table 5. Hazard Quotients (HQ) and Hazard Index (HI) for settleable particulate matter (SPM), indoor dust (ID) and surface soils. Because Cu yielded very high HQ values in SPM and ID and would dominate screening totals, HI and ΣHI are reported excluding Cu to facilitate interpretation of the remaining metals. Total HI including Cu can be obtained as $HI_{total} = HI + HQ_{Cu}$. Seasonal averages were used to estimate the confidence levels for each site, and these are available in Supplementary Table S9.

Sample site	As	Cd	Cr	Cu	Ni	Pb	Hazard Index*	Overall for study zone*
	Hazard Quotient (HQ)						HI	Σ HI
PW1	0.70	0.26	0.19	15	0.03	1.23	2.42	21
PW2	0.52	0.13	0.15	14	0.02	0.57	1.39	
PW3	0.79	0.19	0.16	47	0.02	1.16	2.32	
PW4	0.71	0.34	0.19	28	0.03	2.24	4	
PW5	1.64	1.26	0.48	38	0.06	3	6	
PW6	0.98	0.55	0.44	45	0.05	3	5	
PS1	0.81	0.25	0.19	5	0.04	0.51	1.80	73
PS2	1.81	0.60	0.36	11	0.03	1.27	4	
PS3	1.82	0.55	0.37	34	0.02	0.96	4	
PS4	1.37	0.52	0.40	9	0.03	0.93	3	
PS5	7	3	2.60	49	0.19	8	21	
PS6	17	7	3	137	0.40	12	39	
DW1	0.14	0.02	0.04	1.52	4.5·10 ⁻³	0.45	0.66	5
DW2	0.16	0.02	0.05	2.14	0.01	0.27	0.51	
DW3	0.39	0.02	0.05	9	0.01	0.57	1.04	
DW4	0.17	0.01	0.05	3	4.1·10 ⁻³	0.23	0.47	
DW5	0.23	0.01	0.04	3	4.6·10 ⁻³	0.21	0.49	
DW6	0.55	0.02	0.09	8	0.02	0.75	1.42	
DS1	0.27	0.02	0.04	4.81	5.1·10 ⁻³	0.61	0.93	6
DS2	0.16	0.01	0.30	2.79	0.01	0.42	0.90	
DS3	0.36	0.02	0.05	9	0.01	0.59	1.03	
DS4	0.19	0.01	0.05	4	4.7·10 ⁻³	0.70	0.95	
DS5	0.33	0.01	0.05	9	4.3·10 ⁻³	0.54	0.94	
DS6	0.28	0.03	0.04	3	0.01	0.91	1.27	

S1	0.04 ± 0.01	0.01 ± 9.7·10 ⁻⁴	0.02 ± 0.01	0.29 ± 0.15	1.3·10 ⁻³ ± 3.7·10 ⁻⁴	0.07 ± 0.04	0.43 ± 0.16	2.33 ± 0.73
S2	0.06 ± 0.02	0.01 ± 5.8·10 ⁻⁴	0.01 ± 6.6·10 ⁻⁴	0.58 ± 0.10	8.2·10 ⁻⁴ ± 1.3·10 ⁻⁴	0.05 ± 0.03	0.71 ± 0.11	
S3	0.04 ± 0.01	3.4·10 ⁻³ ± 7.9·10 ⁻⁴	0.01 ± 4.0·10 ⁻³	0.71 ± 0.68	8.9·10 ⁻⁴ ± 2.9·10 ⁻⁴	0.07 ± 0.02	0.84 ± 0.68	
S4	0.02 ± 3.7·10 ⁻³	2.1·10 ⁻³ ± 8.0·10 ⁻⁴	0.01 ± 1.2·10 ⁻³	0.28 ± 0.19	9.0·10 ⁻⁴ ± 3.1·10 ⁻⁴	0.05 ± 0.01	0.35 ± 0.19	

HI and ΣHI were calculated excluding Cu for SPM and indoor settled dust; Cu HQ values are reported separately.

Table 6. Incremental Lifetime Cancer Risk (ILCR) and *Risk* Index for settleable particulate matter (SPM), indoor dust (ID), and surface soils (S) in schools of the Quintero–Puchuncaví district. Risks are interpreted against USEPA thresholds (10⁻⁶–10⁻⁴), where values above 10⁻⁴ indicate “probable cancer risk” scenarios. Seasonal averages were used to estimate the confidence levels for each site, and these are available in Supplementary Table S9.

Sampl e- site	As	Cd	Cr	Ni	Pb	Risk index	Overall, for study zone*
	Incremental Lifetime Cancer Risk (ILCR)					Risk	ΣRisk
PW1	2.0·10 ⁻⁵	2.3·10 ⁻⁹	1.6·10 ⁻⁵	5.6·10 ⁻⁵	3.0·10 ⁻⁷	9.2·10 ⁻⁵	7.5·10 ⁻⁴
PW2	1.5·10 ⁻⁵	1.1·10 ⁻⁹	1.2·10 ⁻⁵	3.5·10 ⁻⁵	1.4·10 ⁻⁷	6.2·10 ⁻⁵	
PW3	2.3·10 ⁻⁵	1.6·10 ⁻⁹	1.3·10 ⁻⁵	4.7·10 ⁻⁵	2.8·10 ⁻⁷	8.2·10 ⁻⁵	
PW4	2.0·10 ⁻⁵	3.0·10 ⁻⁹	1.5·10 ⁻⁵	7.5·10 ⁻⁵	5.5·10 ⁻⁷	1.1·10 ⁻⁴	
PW5	4.7·10 ⁻⁵	1.1·10 ⁻⁸	3.9·10 ⁻⁵	1.4·10 ⁻⁴	6.8·10 ⁻⁷	2.2·10 ⁻⁴	
PW6	2.8·10 ⁻⁵	4.7·10 ⁻⁹	3.5·10 ⁻⁵	1.2·10 ⁻⁴	7.7·10 ⁻⁷	1.8·10 ⁻⁴	
PS1	2.3·10 ⁻⁵	2.2·10 ⁻⁹	1.6·10 ⁻⁵	8.1·10 ⁻⁵	1.2·10 ⁻⁷	1.2·10 ⁻⁴	3.1·10 ⁻³
PS2	5.2·10 ⁻⁵	5.2·10 ⁻⁹	3.0·10 ⁻⁵	7.6·10 ⁻⁵	3.1·10 ⁻⁷	1.6·10 ⁻⁴	
PS3	5.2·10 ⁻⁵	4.8·10 ⁻⁹	3.1·10 ⁻⁵	5.4·10 ⁻⁵	2.4·10 ⁻⁷	1.4·10 ⁻⁴	
PS4	3.9·10 ⁻⁵	4.5·10 ⁻⁹	3.3·10 ⁻⁵	7.2·10 ⁻⁵	2.3·10 ⁻⁷	1.4·10 ⁻⁴	
PS5	2.0·10 ⁻⁴	2.8·10 ⁻⁸	2.2·10 ⁻⁴	4.3·10 ⁻⁴	1.9·10 ⁻⁶	8.5·10 ⁻⁴	
PS6	4.9·10 ⁻⁴	5.8·10 ⁻⁸	2.9·10 ⁻⁴	8.9·10 ⁻⁴	2.9·10 ⁻⁶	1.7·10 ⁻³	
DW1	3.5·10 ⁻⁶	4.3·10 ⁻¹⁰	2.8·10 ⁻⁶	8.7·10 ⁻⁶	1.0·10 ⁻⁷	1.5·10 ⁻⁵	1.7·10 ⁻⁴

DW2	$3.9 \cdot 10^{-6}$	$4.6 \cdot 10^{-10}$	$3.2 \cdot 10^{-6}$	$2.0 \cdot 10^{-5}$	$5.9 \cdot 10^{-8}$	$2.7 \cdot 10^{-5}$	
DW3	$9.4 \cdot 10^{-6}$	$4.2 \cdot 10^{-10}$	$3.3 \cdot 10^{-6}$	$1.9 \cdot 10^{-5}$	$1.1 \cdot 10^{-7}$	$3.2 \cdot 10^{-5}$	
DW4	$4.9 \cdot 10^{-6}$	$3.8 \cdot 10^{-10}$	$4.0 \cdot 10^{-6}$	$9.4 \cdot 10^{-6}$	$5.7 \cdot 10^{-8}$	$1.8 \cdot 10^{-5}$	
DW5	$6.6 \cdot 10^{-6}$	$3.0 \cdot 10^{-10}$	$3.4 \cdot 10^{-6}$	$1.0 \cdot 10^{-5}$	$5.2 \cdot 10^{-8}$	$2.1 \cdot 10^{-5}$	
DW6	$1.6 \cdot 10^{-5}$	$5.4 \cdot 10^{-10}$	$7.5 \cdot 10^{-6}$	$3.5 \cdot 10^{-5}$	$1.9 \cdot 10^{-7}$	$5.9 \cdot 10^{-5}$	
DS1	$3.7 \cdot 10^{-5}$	$4.1 \cdot 10^{-10}$	$3.7 \cdot 10^{-6}$	$1.2 \cdot 10^{-5}$	$1.2 \cdot 10^{-7}$	$5.2 \cdot 10^{-5}$	$3.9 \cdot 10^{-4}$
DS2	$1.7 \cdot 10^{-5}$	$3.4 \cdot 10^{-10}$	$3.1 \cdot 10^{-5}$	$3.6 \cdot 10^{-5}$	$8.1 \cdot 10^{-8}$	$8.5 \cdot 10^{-5}$	
DS3	$5.0 \cdot 10^{-5}$	$4.7 \cdot 10^{-10}$	$5.0 \cdot 10^{-6}$	$1.9 \cdot 10^{-5}$	$1.1 \cdot 10^{-7}$	$7.3 \cdot 10^{-5}$	
DS4	$2.8 \cdot 10^{-5}$	$3.4 \cdot 10^{-10}$	$5.8 \cdot 10^{-6}$	$1.3 \cdot 10^{-5}$	$1.7 \cdot 10^{-7}$	$4.7 \cdot 10^{-5}$	
DS5	$5.0 \cdot 10^{-5}$	$4.4 \cdot 10^{-10}$	$5.1 \cdot 10^{-6}$	$1.1 \cdot 10^{-5}$	$1.4 \cdot 10^{-7}$	$6.7 \cdot 10^{-5}$	
DS6	$4.2 \cdot 10^{-5}$	$1.1 \cdot 10^{-9}$	$4.2 \cdot 10^{-6}$	$2.1 \cdot 10^{-5}$	$2.3 \cdot 10^{-7}$	$6.7 \cdot 10^{-5}$	
S1	$1.1 \cdot 10^{-6} \pm 1.9 \cdot 10^{-7}$	$2.2 \cdot 10^{-10} \pm 2.5 \cdot 10^{-11}$	$1.1 \cdot 10^{-6} \pm 7.3 \cdot 10^{-7}$	$2.7 \cdot 10^{-6} \pm 7.6 \cdot 10^{-7}$	$1.6 \cdot 10^{-8} \pm 8.2 \cdot 10^{-9}$	$4.9 \cdot 10^{-6} \pm 1.1 \cdot 10^{-6}$	$1.6 \cdot 10^{-5} \pm 1.6 \cdot 10^{-6}$
S2	$1.6 \cdot 10^{-6} \pm 5.3 \cdot 10^{-7}$	$1.4 \cdot 10^{-10} \pm 1.7 \cdot 10^{-11}$	$7.6 \cdot 10^{-7} \pm 4.1 \cdot 10^{-7}$	$1.7 \cdot 10^{-6} \pm 1.9 \cdot 10^{-7}$	$1.2 \cdot 10^{-8} \pm 4.4 \cdot 10^{-9}$	$4.1 \cdot 10^{-6} \pm 7.0 \cdot 10^{-7}$	
S3	$1.2 \cdot 10^{-6} \pm 3.3 \cdot 10^{-7}$	$9.0 \cdot 10^{-11} \pm 1.7 \cdot 10^{-11}$	$7.2 \cdot 10^{-7} \pm 3.0 \cdot 10^{-7}$	$1.9 \cdot 10^{-6} \pm 5.9 \cdot 10^{-7}$	$1.7 \cdot 10^{-8} \pm 4.6 \cdot 10^{-9}$	$3.8 \cdot 10^{-6} \pm 7.3 \cdot 10^{-7}$	
S4	$6.7 \cdot 10^{-7} \pm 1.0 \cdot 10^{-7}$	$5.5 \cdot 10^{-11} \pm 2.1 \cdot 10^{-11}$	$4.8 \cdot 10^{-7} \pm 8.7 \cdot 10^{-8}$	$1.9 \cdot 10^{-6} \pm 6.4 \cdot 10^{-7}$	$1.0 \cdot 10^{-8} \pm 2.7 \cdot 10^{-9}$	$3.0 \cdot 10^{-6} \pm 6.5 \cdot 10^{-7}$	

3.4. International Context and Comparisons

Evidence from Chilean studies around the Ventanas industrial complex is consistent with the enrichment patterns observed here [18-22]. Independent surveys of topsoils, vegetation, and atmospheric deposition in the district document spatial gradients of Cu, Pb, and Cd associated with proximity to industrial sources and prevailing transport pathways [18-21], which explains the impact of Cu in SPM and dust, after the closure of CODELCO Cu smelting. These studies also characterize contaminated surface soils as persistent metal reservoirs in fine fractions, which supports the plausibility of soil-driven resuspension contributing to settled dust and deposited particulate matter [18, 39]. Recent school-focused work in the same district reported elevated metals in educational microenvironments and quantified screening risks, reinforcing the relevance of schools as an exposure setting [22]. Within the broader framing of environmental sacrifice zones, these convergent findings indicate that schools and surrounding residential areas can experience chronic exposure pressures even when regulations target point-source emissions [15, 16].

Comparable dust- and soil-based assessments in industrial and mining-impacted settings show that near-surface dust can act as an integrative sink for metal emissions and resuspended contaminated soils, frequently motivating screening health risk evaluations [5-8]. Street dust in Luanda, Angola shows that tropical urban environments can accumulate elevated TMs and generate non-carcinogenic and carcinogenic risk estimates under standardized exposure assumptions [5]. Similarly, smelter-influenced urban dust in Northeast China exhibited high metal loads and associated health risks, supporting the applicability of dust-based screening across smelter-affected regions [6]. In Kabwe, Zambia, widespread soil contamination by Cu, Pb, Cd, and Zn persists and supplies material for dust generation and human exposure [7]. Biomonitoring in the Katanga mining belt reports high human exposure to cobalt and other metals, indicating that environmental contamination results in measurable internal doses near mining and smelting operations [8].

School-based dust studies in large cities further support the use of indoor and outdoor dust as exposure-relevant matrices for children who spend substantial time in classrooms. In Riyadh, Saudi Arabia, heavy metals in elementary-school dust were assessed using pollution indices and screening risk metrics, establishing an international benchmark for school-based evaluations [40]. Urban traffic-dust studies likewise indicate that resuspended road dust transports metal mixtures contributing to non-carcinogenic and carcinogenic screening metrics in densely populated settings [45]. Because settled dust integrates infiltration, deposition, and resuspension, its metal burdens have been associated with PM₁₀ concentrations and personal inhalation exposure, although translation to airborne doses remains uncertain [49]. The intermediate contamination of indoor dust relative to SPM and soils is consistent with an outdoor-to-indoor pathway governed by particle deposition and resuspension [3, 49].

From a public-health perspective, WHO identifies particulate air pollution as a leading environmental risk factor and has tightened guideline levels for PM_{2.5} and PM₁₀ to better protect vulnerable groups [9, 10]. For lead, the CDC emphasizes that no safe blood lead level has been identified in children and has lowered the blood lead reference value, highlighting the need to minimize Pb-bearing dust exposure in schools [11]. Within the U.S. EPA risk-assessment framework, hazard indices and cancer risks support screening and prioritization of further evaluation, with regional screening levels providing consistent interpretive benchmarks [23, 24, 43]. Under this screening framework, summer exceedances at inland valley schools indicate that school microenvironments in industrial coastal basins require targeted follow-up monitoring and exposure-reduction measures focused on deposited and resuspended dust [23, 24].

These results provide screening evidence that metal-rich deposited particles and indoor settled dust can constitute relevant exposure media in schools located within topographically constrained industrial coastal basins, with the highest risks observed at inland valley schools during summer.

3.5. Study Limitations, Strengths, and Recommendations

A key strength of this work is its multi-matrix design, which jointly evaluates surface soils, indoor settled dust, and settleable particulate matter, thereby supporting an integrated interpretation of contaminant reservoirs, indoor accumulation, and deposition-linked exposure pathways. Because EF and Igeo depend on background selection, we anchored both indices to a locally derived geochemical baseline estimated using a robust median absolute deviation approach [38, 39]. Integrating geochemical indexing with a transparent, screening-level HRA framework provides a practical basis for prioritization while maintaining comparability with prior dust-based risk assessments [5, 23, 24].

This study also establishes a clear foundation for subsequent refinement and expansion. The dataset offers a focused, policy-relevant snapshot across six schools, with two seasonal campaigns for dust and SPM and a winter soil survey, which is sufficient to detect consistent contrasts among matrices and to identify priority locations and seasons for follow-up. Screening risk estimates are derived from total metal concentrations and default exposure factors that are widely used for prioritization and benchmarking, while acknowledging that site-specific behaviors, time-activity

patterns, and building operations can further modulate exposure in real settings [23-26]. For inhalation, deposited SPM must be related to airborne concentrations, and building and exposure studies indicate that the correspondence between settled dust and PM₁₀-bound metal exposures can vary across microenvironments and operating conditions; paired measurements therefore represent a straightforward next step to further constrain inhalation estimates [49]. Finally, although speciation and bio accessibility were beyond the scope of the present campaign, incorporating these measurements in future work would refine toxicity-relevant dose estimates for metals with form-dependent hazards, particularly As and Cr [50].

From a risk-management perspective, screening exceedances provide a defensible basis to prioritize targeted monitoring and mitigation at schools using established benchmark frameworks, including U.S. EPA regional screening levels and associated risk-assessment guidance [23, 24, 43]. Follow-up campaigns would benefit from paired settled-dust, deposition, and airborne PM measurements, including size-resolved sampling, to reduce uncertainty in inhalation exposure estimates [49]. Where feasible, source-apportionment approaches and Pb isotope signatures can help distinguish industrial contributions from traffic-related inputs to deposited particles [47]. At the school level, exposure reduction is likely to be most effective when control of outdoor dust ingress is coupled with cleaning protocols that minimize indoor resuspension, consistent with established indoor particle dynamics [3]. At the regulatory level, explicitly incorporating school microenvironments into air-quality management, surveillance, and risk communication aligns with WHO guidance emphasizing the protection of vulnerable populations from particulate pollution [9, 10]. Because no safe level of lead exposure has been identified for children, reducing Pb-bearing dust in educational settings remains a clear public-health priority [11].

5. Conclusions

This work presents a screening multi-matrix assessment of trace metals in school environments within an industrial coastal basin in central Chile. The environmental impact index provides evidence of the severe impact in the area, Settleable particulate matter (SPM) exhibited the highest concentrations and enrichment, with EF and Igeo indicating strong anthropogenic influence at several sites. Seasonal contrasts were evident, with higher summer burdens of As, Cd, Cr, and Ni in SPM and, to a lesser extent, indoor dust. Although soils were generally less enriched, they represent longer-term reservoirs that can sustain resuspension, while indoor dust functions as an intermediate medium that transfers outdoor contamination into classrooms.

Health risk assessment offered valued insight in the risk for exposure to the matrices studied throughout the zone. Under the U.S. EPA screening framework, Cu dominated non-carcinogenic hazard (HQ up to 137), whereas ILCR was driven mainly by Ni, As, and Cr, exceeding 10^{-4} and reaching 10^{-3} at inland schools in summer. Indoor dust produced intermediate hazard and risk, reinforcing the need to account for indoor accumulation when evaluating children's exposures.

Furthermore, this study highlights the importance of the results obtained from the Los Maquis and Pucalan sectors. Which showed the highest TE concentrations across all sample types, and the overall highest EF, Igeo, HQ, HI, ILCR and Risk indexes. These results showcase the importance of assessing the impact area of a sacrifice zone or an industry objectively, minimizing or eliminating any potential bias. Notably, these two sectors are not traditionally considered part of the affected area, this may be attributed to their lower population compared to the sectors of Quintero and Puchuncaví. Nevertheless, the findings indicate that some of the most potentially vulnerable populations may reside in areas that are often overlooked. Geographic factors should be considered when delineating the area for a health risk assessment, as the consistently elevated TMs concentrations obtained in all samples in Los Maquis and Pucalan, may be attributed to their specific geographic characteristics and serve as early indicators of potential exposure risk.

Finally, the multi-matrix evidence indicates that deposited particles and indoor dust can constitute relevant exposure media in school environments within industrial coastal basins, supporting confirmatory monitoring and risk-management evaluation in the most affected settings.

Author Contributions: F.G.V: Conceptualization, Data curation, Formal analysis, Investigation, Validation, Methodology, Writing—original draft, Writing—review and editing. F.L.O.: Data curation, Formal analysis, Methodology. C.C.S.: Data curation, Methodology. A.V.D: Methodology, Investigation, writing—review and editing. M.A.L.G.: Conceptualization, Methodology, Investigation, Validation, Funding acquisition, Supervision, Visualization, Writing—original draft. R.T.A: Conceptualization, Methodology, Investigation, Validation, Funding acquisition, Supervision, Visualization, Writing—review and editing.

Funding: This research was partially supported by the Chilean National Fund for Scientific and Technological Development (FONDECYT), under ANID FONDECYT Regular Grants No. 1220948 and 1241485.

Data Availability Statement: The datasets supporting the conclusions of this article are available from the corresponding author upon reasonable request for academic, non-commercial research purposes. Any reuse of the data must include appropriate attribution to the original data providers and to this article, in accordance with Elsevier's data sharing and citation policies.

Acknowledgments: The authors thank the laboratory team for their valuable contributions during the development of the study and to the refinement of the methodological framework through extensive and constructive discussions.

Conflicts of Interest: The authors declare no conflicts of interest.

References

1. L.C. Chen, M. Lippmann, Effects of Metals within Ambient Air Particulate Matter (PM) on Human Health, *Inhalation Toxicology* 21 (2009) 1-31.
2. S.A. Weichenthal, K. Godri Pollitt, P.J. Villeneuve, PM_{2.5}, oxidant defence and cardiorespiratory health: a review, *Environmental Health* 12 (2013) 40.
3. W.W. Nazaroff, Indoor particle dynamics, *Indoor Air* 14 (2004) 175-183.
4. H.W. Mielke, P.L. Reagan, Soil is an important pathway of human lead exposure, *Environ Health Perspect* 106 Suppl 1 (1998) 217-229.
5. L. Ferreira-Baptista, E. De Miguel, Geochemistry and risk assessment of street dust in Luanda, Angola: A tropical urban environment, *Atmospheric Environment* 39 (2005) 4501-4512.
6. X. Qing, Z. Yutong, L. Shenggao, Assessment of heavy metal pollution and human health risk in urban soils of steel industrial city (Anshan), Liaoning, Northeast China, *Ecotoxicology and Environmental Safety* 120 (2015) 377-385.
7. B.D. Tembo, K. Sichilongo, J. Cernak, Distribution of copper, lead, cadmium and zinc concentrations in soils around Kabwe town in Zambia, *Chemosphere* 63 (2006) 497-501.
8. C.L.N. Banza, T.S. Nawrot, V. Haufroid, S. Decrée, T. De Putter, E. Smolders, B.I. Kabyla, O.N. Luboya, A.N. Ilunga, A.M. Mutombo, B. Nemery, High human exposure to cobalt and other metals in Katanga, a mining area of the Democratic Republic of Congo, *Environmental Research* 109 (2009) 745-752.
9. WHO, Guidelines Approved by the Guidelines Review Committee, WHO global air quality guidelines: Particulate matter (PM_{2.5}) and PM₁₀), ozone, nitrogen dioxide, sulfur dioxide and carbon monoxide, World Health Organization © World Health Organization 2021., Geneva, 2021.
10. WHO, Ambient (outdoor) air pollution, World Health Organization, 2024.
11. CDC, CDC Updates Blood Lead Reference Value, Centers for Disease Control and Prevention, 2024.
12. S. Lerner, *Sacrifice Zones. The Front Lines of Toxic Chemical Exposure in the United States*, The MIT Press 2010.
13. R.D. Bullard, Book Review. *Sacrifice Zones: The Front Lines of Toxic Chemical Exposure in the United States*, *Environmental Health Perspectives* 116 (2011).
14. D. Cabezas, *Zonas de sacrificio: qué son, dónde están y por qué suponen un desastre ecológico*, Los40, 2023.

15. E.M. Gayo, A.A. Muñoz, A. Maldonado, C. Lavergne, J.P. Francois, D. Rodríguez, K. Klock-Barría, P.R. Sheppard, I. Aguilera-Betti, C. Alonso-Hernández, M. Mena-Carrasco, A. Urquiza, L. Gallardo, A Cross-Cutting Approach for Relating Anthropocene, Environmental Injustice and Sacrifice Zones, *Earth's Future* 10 (2022) e2021EF002217.
16. K. Valenzuela-Fuentes, E. Alarcón-Barrueto, R. Torres-Salinas, From Resistance to Creation: Socio-Environmental Activism in Chile's "Sacrifice Zones", *Sustainability*, 2021, pp. 3481.
17. N. Palma, Entre el progreso y la crisis medioambiental: Fundación Ventanas inició cierre de operaciones tras 58 años de actividad, *Radio Universidad de Chile* Chile, 2023.
18. I. González, A. Neaman, P. Rubio, A. Cortés, Spatial distribution of copper and pH in soils affected by intensive industrial activities in Puchuncaví and Quintero, central Chile, *Journal of soil science and plant nutrition* 14 (2014) 943-953.
19. S. Parra, M.A. Bravo, W. Quiroz, T. Moreno, A. Karanasiou, O. Font, V. Vidal, F. Cereceda, Distribution of trace elements in particle size fractions for contaminated soils by a copper smelting from different zones of the Puchuncaví Valley (Chile), *Chemosphere* 111 (2014) 513-521.
20. F. Rueda-Holgado, L. Calvo-Blázquez, F. Cereceda-Balic, E. Pinilla-Gil, Temporal and spatial variation of trace elements in atmospheric deposition around the industrial area of Puchuncaví-Ventanas (Chile) and its influence on exceedances of lead and cadmium critical loads in soils, *Chemosphere* 144 (2016) 1788-1796.
21. J. Tapia-Gatica, I. González-Miranda, E. Salgado, M.A. Bravo, C. Tessini, E.A. Dovletyarova, A.A. Paltseva, A. Neaman, Advanced determination of the spatial gradient of human health risk and ecological risk from exposure to As, Cu, Pb, and Zn in soils near the Ventanas Industrial Complex (Puchuncaví, Chile), *Environmental Pollution* 258 (2020) 113488.
22. S. Parra, H. de la Fuente-Mella, A. González-Rojas, M.A. Bravo, Exposure to Environmental Pollution in Schools of Puchuncaví, Chile: Characterization of Heavy Metals, Health Risk Assessment, and Effects on Children's Academic Performance, *Sustainability*, 2024, pp. 2518.
23. [23] U.S. EPA, Risk assessment guidance for Superfund: Volume 1 - Human health evaluation manual. Part E, Supplemental Guidance for Dermal Risk Assessment, in: O.o.S.R.a.T. Innovation (Ed.) United States, 2004.
24. U.S. EPA, Risk assessment guidance for Superfund: Volume 1 - Human health evaluation manual. Part F, Supplemental Guidance for Inhalation Risk Assessment, United States, 2009.
25. U.S. EPA, Exposure Factors Handbook 2011 Edition (Final Report), United States, 2011.
26. U.S. EPA, Update for Chapter 5 of the Exposure Factors Handbook: Soil and dust ingestion, United States, 2017.
27. D.G.d.A.C. DGAC Chile, & DMC, (Dirección Meteorológica de Chile - Servicios Climáticos), Agua Caída, Valores diarios, mensuales y totales para un año, 2024.
28. A. Richard Toro, A. Tomás Claramunt, V. Fiorella González, G. Sebastián Ávila, A.L.-G. Manuel, Long-term assessment and acute air pollution events in a mega-industrial area in Central Chile, *Urban Climate* 55 (2024) 101880.
29. C. Oyarzo-Miranda, N. Latorre, A. Meynard, J. Rivas, C. Bulboa, L. Contreras-Porcía, Coastal pollution from the industrial park Quintero bay of central Chile: Effects on abundance, morphology, and development of the kelp *Lessonia spicata* (Phaeophyceae), *PLOS ONE* 15 (2020) e0240581.
30. J.O. Anderson, J.G. Thundiyil, A. Stolbach, Clearing the Air: A Review of the Effects of Particulate Matter Air Pollution on Human Health, *Journal of Medical Toxicology* 8 (2012) 166-175.
31. A. Garcia, E. Santa-Helena, A. De Falco, J. de Paula Ribeiro, A. Gioda, C.R. Gioda, Toxicological Effects of Fine Particulate Matter (PM_{2.5}): Health Risks and Associated Systemic Injuries—Systematic Review, *Water, Air, & Soil Pollution* 234 (2023) 346.
32. F. Lobos, Tasas de deposición de metales pesados asociados al material particulado sedimentable en el entorno del Complejo Industrial Las Ventanas University of Chile, 2024.
33. U.S. EPA, Method 3051A (SW-846): Microwave Assisted Acid Digestion of Sediments, Sludges, and Oils, United States, 2007.
34. E.J. dos Santos Souza, C. Zapata Mora, B.H. Aristizábal Zuluaga, C.D. Britto do Amaral, M.T. Grassi, Multi-elemental analysis of particulate matter PM_{2.5} and PM₁₀ by ICP OES, *Talanta* 221 (2021) 121457.

35. R.A. Sutherland, Bed sediment-associated trace metals in an urban stream, Oahu, Hawaii, *Environmental Geology* 39 (2000) 611-627.
36. G. Muller, INDEX OF GEOACCUMULATION IN SEDIMENTS OF THE RHINE RIVER, *GeoJournal* 2 (1969) 108-118.
37. K. Loska, D. Wiechuła, I. Korus, Metal contamination of farming soils affected by industry, *Environment International* 30 (2004) 159-165.
38. M. Barbieri, The Importance of Enrichment Factor (EF) and Geoaccumulation Index (Igeo) to Evaluate the Soil Contamination, *Journal of Geology & Geophysics* 5 (2016) 1-4.
39. V. Zapata Aguiló, Análisis geoquímico y geoestadístico de la concentración elemental en los suelos de las comunas de Quintero y Puchuncaví, University of Chile, 2020.
40. M.O. Alotaibi, L.A. Albedair, N.M. Alotaibi, M.M. Elobeid, H.A. Al-Swadi, Z. Alasmay, M. Ahmad, Pollution Indexing and Health Risk Assessment of Heavy-Metals-Laden Indoor and Outdoor Dust in Elementary School Environments in Riyadh, Saudi Arabia, *Atmosphere*, 2022, pp. 464.
41. C. Instituto Nacional de Estadísticas, Proyecciones y Estimaciones de Población. Esperanza de vida al nacer (en años), según sexo, por quinquenios comprendidos entre los años 1950 y 2025., Instituto Nacional de Estadísticas (INE) de Chile., 2004.
42. A. Parviainen, A. Vázquez-Arias, J.P. Arrebola, F.J. Martín-Peinado, Human health risks associated with urban soils in mining areas, *Environmental Research* 206 (2022) 112514.
43. U.S. EPA, Regional Screening Levels (RSLs) - Generic Tables, United States Environmental Protection Agency United States, 2015.
44. R.A.I.S. (RAIS). Chemical Toxicity Values, Oak Ridge National Laboratory, 2024.
45. N. Mahmoud, D. Al-Shahwani, H. Al-Thani, R.J. Isaifan, Risk Assessment of the Impact of Heavy Metals in Urban Traffic Dust on Human Health, *Atmosphere*, 2023, pp. 1049.
46. M. Alsafran, K. Usman, H. Al Jabri, M. Rizwan, Ecological and Health Risks Assessment of Potentially Toxic Metals and Metalloids Contaminants: A Case Study of Agricultural Soils in Qatar, *Toxics*, 2021, pp. 35.
47. A. Bollhöfer, K.J.R. Rosman, Isotopic source signatures for atmospheric lead: the Southern Hemisphere, *Geochimica et Cosmochimica Acta* 64 (2000) 3251-3262.
48. Arsenic, metals, fibres, and dusts, IARC Monogr Eval Carcinog Risks Hum 100 (2012) 11-465.
49. P.E. Rasmussen, C. Levesque, M. Chénier, H.D. Gardner, Contribution of metals in resuspended dust to indoor and personal inhalation exposures: Relationships between PM10 and settled dust, *Building and Environment* 143 (2018) 513-522.
50. IARC, Arsenic, metals, fibres, and dusts, IARC Monogr Eval Carcinog Risks Hum 100 (2012) 11-465.

Disclaimer/Publisher's Note: The statements, opinions and data contained in all publications are solely those of the individual author(s) and contributor(s) and not of MDPI and/or the editor(s). MDPI and/or the editor(s) disclaim responsibility for any injury to people or property resulting from any ideas, methods, instructions or products referred to in the content.